Available online at www.sciencedirect.com
ScienceDirect
European Journal of Mechanics B/Fluids 27 (2008) 346–360

Short crested wave–current forces around a large vertical circular cylinder

Yongjun Jian [a,b,*], Jiemin Zhan [a,b,c], Qingyong Zhu [a,b]

[a] *Ocean Engineering Research Center, School of Engineering, Zhongshan University, Guangzhou, 510275, China*
[b] *Guangdong Province Key Laboratory of Coastal Ocean Engineering, Zhongshan University, Guangzhou, 510275, China*
[c] *Department of Applied Mechanics and Engineering, Zhongshan University, Guangzhou, 510275, China*

Received 2 January 2007; received in revised form 8 August 2007; accepted 8 August 2007

Available online 14 August 2007

Abstract

An analytical solution for the diffraction of short crested incident wave along positive x-axis direction on a large circular cylinder with uniform current is derived. The important influences of currents on wave frequency, water run-up, wave force, inertia and drag coefficients on the cylinder profiles are investigated for short-crested incident wave. Based on the numerical results, we find wave frequency of short crested wave system is affected by incident angle and the strength of the currents. The wave frequency increases or decreases with increasing current speed following or opposing wave propagating direction. It shows that the effects of current speeds, current directions on water run-up on the circular cylinder with different radius for different wave numbers are very conspicuous when the incident wave changes from long crested plane waves to short-crested waves. With the increase of current speed, the water run-up on the cylinder becomes more and more high, and will exceed that of long crested plane wave and short crested wave case without currents even though the current speed is small. The total wave loads, inertia coefficient and drag coefficient exerted on a cylinder with currents would be larger compared to the wave loads exerted pure short-crested waves. Therefore, ocean engineers should consider the short crested wave–current load on marine constructs carefully.

Keywords: Short crested wave; Uniform currents; Water run-up on the cylinder; Wave force

1. Introduction

Vertical circular cylinders are used in many oceanographic applications such as buoys, drilling rigs and instrumentation platforms for their simplicity in construction. Ocean wave are the dominant form of hydrodynamic loading generally encountered in the offshore environment. The wave forces exerted on slender bodies due to regular waves is generally evaluated based on the formulation proposed by Morison et al. [1]. The Morison equation was formulated with the assumption that the presence of the object did not affect the characteristics of the incident wave field. However, this formulation fails to predict the wave induced forces on large diameter structures where the effects of the scattering of waves from the structure are predominant and a diffraction theory must be employed to compute the

* Corresponding author at: Ocean Engineering Research Center, School of Engineering, Zhongshan University, Guangzhou, 510275, China.
E-mail address: jianyongjun@yahoo.com.cn (Y. Jian).

0997-7546/$ – see front matter
doi:10.1016/j.euromechflu.2007.08.001

forces exerted on the structure by the scattered waves. The determination of wave forces on large offshore structures is quite complex mainly because of the scattering of the waves in the vicinity of the structure. Furthermore, the presence of an ocean current may drastically alter the wave conditions. Although the effects of wave–current interaction are more dramatic for strong currents, it has been found that even the relatively weak currents of the open ocean exert an appreciable influence on the properties of gravity waves, causing changes in the wavelength, amplitude, direction of propagation and energy density spectrum.

MacCamy and Fuchs [2] arrived at a closed form solution to evaluate the dynamic pressures, forces and moments on a single large vertical circular cylinder subjected to linear plane waves being diffracted around a large vertical cylinder. Their results have been proved both by experiments [3,4] and numerical models [5,6]. However, the co-existence of waves and currents is a common feature of most marine environments. The Morison formula has been used by Tung and Huang [7] to determine the effect of wave–current interactions on the fluid force exerted on cylindrical elements which are small relative to the incident waves. Watanabe [8] investigated the effect of wave–current interactions on the fluid loading of large offshore structures by extending the conventional diffraction theory approach to include the changes in the incident and scattered wave fields caused by the presence of a steady current.

In fact, most wind-generated waves in oceans are much better modeled by short-crested waves than by plane waves, and short-crested waves have many different properties compared to a long-crested plane waves. Hsu et al. [9] calculated a third order short-crested wave solution in non-dimensional form using an expansion parameter related to the ratio of the waveheight to the wavelength of the incident wave, including the standing wave limit. Silvester [10] considered the influence of oblique short-crested wave reflection on breakwater. In real oceanic environments, the short crested wave fields ordinary are coupled with currents. Recently, Huang and Jia [11] studied the patterns of capillary gravity short crested waves with uniform current. They obtained second order approximate solutions and gave some results for the wave profiles with and without currents. Zhu [12] carried out the study on the diffraction of short-crested waves on a circular cylinder and found that wave loads induced by short-crested waves on a circular cylinder are always less than those induced by plane waves with the same total wave number. Thus from the safety point of view, the wave loading formula derived from a plane incident wave may will serve as a good engineering design criterion.

However, no-one seems to have discussed, to the authors' knowledge, the impact of the short-crested waves with a steady uniform current on a large vertical cylinder. One can conjecture that the induced pressure distribution around the cylinder will be different from that induced by pure plane waves and pure short-crested waves due to the presence of a uniform current. It is not clear whether or not the total wave loads exerted on a cylinder would be larger or smaller compared to the wave loads exerted by plane wave–current interactions and pure short-crested waves when the uniform current presents. These problems have a significant influence on the dynamics response of offshore structures and are expected to play an important role in the evaluation of fatigue damage in ocean engineering.

The purpose of this study is mainly to extend Zhu's theory [12] about the diffraction of short-crested waves around a circular cylinder to include the effect of a uniform current for different incident angles. Based on the new solution, the dispersion relation, wave run-up on the cylinder, wave force, inertia coefficient and drag coefficient for different current speeds and incident angles will be examined, which will provide a guide in design of marine structure.

2. Formulation and solution of short crested wave–current forces on a vertical circular cylinder

We consider a train of monochromatic short crested waves of frequency, ω, propagating in the direction of the positive x-axis with a steady uniform current U_0 at an angle β relative to the incident wave direction in an ocean with uniform depth, h, and a fixed vertical circular cylinder of radius, a, which is placed on the floor of the ocean as shown in Fig. 1. We define the right-hand coordinate system O–xyz (or cylindrical coordinate system O–$r\theta z$) so that the origin is placed at the center of circular cylinder on the undisturbed free surface and z points upwards. The fluid is assumed inviscid, incompressible and the motion is irrotational. Therefore, there exists a total velocity potential function Φ, which can be divided into three parts, named as pure current velocity potential $\phi_c(r,\theta,z,t)$, incident short-crested wave velocity potential $\phi_i(r,\theta,z,t)$, and scattered velocity potential $\phi_s(r,\theta,z,t)$.

In cylindrical coordinate system, the total velocity potential Φ satisfies the Laplace equation

$$\Delta\Phi = \frac{\partial^2\Phi}{\partial r^2} + \frac{1}{r}\frac{\partial\Phi}{\partial r} + \frac{1}{r^2}\frac{\partial^2\Phi}{\partial\theta^2} + \frac{\partial^2\Phi}{\partial z^2} = 0 \quad -h \leqslant z \leqslant \eta(r,\theta,t) \tag{2.1}$$

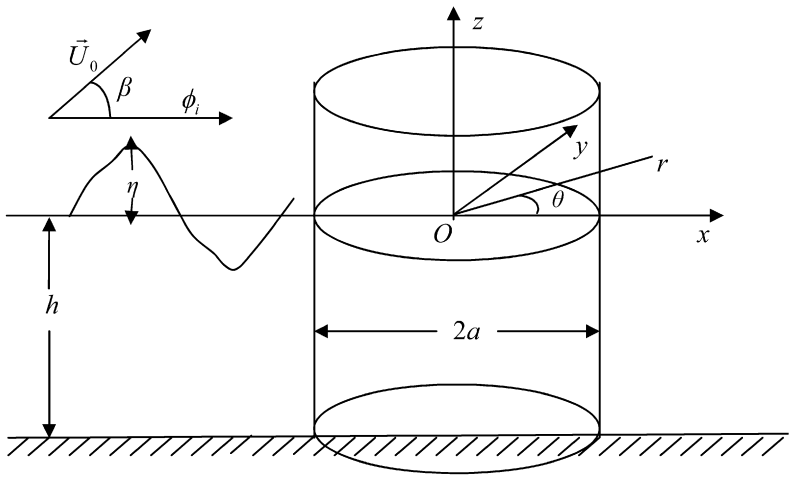

Fig. 1. Definition sketch of short-crested wave–current system around a vertical circular cylinder.

subject to linearized free surface boundary conditions

$$\frac{\partial \Phi}{\partial z} = \frac{\partial \eta}{\partial t} + \vec{U}_0 \cdot \nabla \eta \quad z = 0, \tag{2.2}$$

$$\frac{\partial \Phi}{\partial t} + \vec{U}_0 \cdot \nabla \Phi + g\eta = 0 \quad z = 0. \tag{2.3}$$

Wall condition of the cylinder and sea floor boundary condition are

$$\frac{\partial \Phi}{\partial r} = 0 \quad r = a, \tag{2.4}$$

$$\frac{\partial \Phi}{\partial z} = 0 \quad z = -h, \tag{2.5}$$

where $\vec{U}_0 = (|\vec{U}_0| \cos\beta, |\vec{U}_0| \sin\beta)$ are the uniform current components in x- and y-axis directions respectively, $\eta(r, \theta, t)$ is the water surface elevation, g is gravitational acceleration, r, θ, and z are the cylindrical coordinates, t is the time, and ∇ denotes gradient operator in x–y or r–θ plane. The free surface conditions (2.2) and (2.3) have been linearized for small amplitude, simple harmonic waves and uniform currents.

2.1. Boundary value problem for current only

Following to Ref. [8], the boundary value problem of the flow with a current around a circular cylinder in an incompressible, inviscid fluid and irrotational motion is investigated in this section. The current is assumed to be uniform at infinity with a velocity profile that is constant with depth, and has an angle β relative to the wave propagating direction in positive x-axis. The velocity potential for the current $\phi_c(r, \theta, z, t)$ must satisfy the following differential equation and boundary conditions

$$\Delta \phi_c = \frac{\partial^2 \phi_c}{\partial r^2} + \frac{1}{r}\frac{\partial \phi_c}{\partial r} + \frac{1}{r^2}\frac{\partial^2 \phi_c}{\partial \theta^2} + \frac{\partial^2 \phi_c}{\partial z^2} = 0 \quad -h \leqslant z \leqslant \varsigma_c(r, \theta, t), \tag{2.6}$$

$$\frac{\partial \varsigma_c}{\partial t} + \vec{U}_0 \cdot \nabla \varsigma_c = 0 \quad z = 0, \tag{2.7}$$

$$\frac{p_{\text{atm}}}{\rho} + \vec{U}_0 \cdot \nabla \phi_c + gz = \text{const.} \quad z = 0, \tag{2.8}$$

$$\frac{\partial \phi_c}{\partial r} = 0 \quad r = a, \tag{2.9}$$

$$\frac{\partial \phi_c}{\partial z} = 0 \quad z = -h, \tag{2.10}$$

$$\phi_c(r,\theta) \to |\vec{U}_0| r\cos(\theta-\beta) \quad r\to\infty, \tag{2.11}$$

where $\zeta_c(r,\theta,t)$ is the free surface near cylinder for current only, p_{atm} is atmosphere pressure at the free surface and is supposed to be zero. Similarly, the boundary conditions (2.7) and (2.8) have been linearized. The last condition is deduced as the followings. When $r\to\infty$, the velocity potential of uniform current can be expressed as

$$\phi_c(r,\theta) \to |\vec{U}_0|\cos\beta\cdot x + |\vec{U}_0|\sin\beta\cdot y = |\vec{U}_0|\cos\beta\cdot r\cos\theta + |\vec{U}_0|\sin\beta\cdot r\sin\theta = |\vec{U}_0| r\cos(\theta-\beta).$$

The solution to uniform flow over a circular cylinder is

$$\phi_c = |\vec{U}_0|\left(r+\frac{a^2}{r}\right)\cos(\theta-\beta). \tag{2.12}$$

Substitution of the ϕ_c into the free surface condition (2.8) gives

$$\varsigma_c(r,\theta,t) = -h + \frac{|\vec{U}_0|^2}{2g}\left[1+\frac{2a^2}{r^2} - 2\cos 2(\theta-\beta)\right] \tag{2.13}$$

which indicates that the water level at the cylinder surface remains approximately horizontal for weak currents where

$$|\vec{U}_0|^2 < \frac{2gh}{3-2\cos 2(\theta-\beta)}. \tag{2.14}$$

The solution $\zeta_c(r,\theta,t)$ then approximately satisfies the surface condition given by (2.7).

2.2. Boundary value problem for short-crested waves and currents

For short-crested incident waves traveling in the positive x-direction, the velocity potential can be expressed as

$$\phi_i = -\frac{igA}{\omega^*}\frac{\cosh k(z+h)}{\cosh kh}\exp\bigl[i(k_x x-\omega t)\bigr]\cos(k_y y) \tag{2.15}$$

by using the real part of the solution, in which A is the amplitude of the incident waves, i is imaginary number unit, ω^* is incident wave angular frequency in still water relative to a frame of reference moving with the current U_0, k_x and k_y are the wave number in the x- and y-direction respectively, and k is the total wave number which satisfies

$$k^2 = k_x^2 + k_y^2. \tag{2.16}$$

Elimination of η from (2.2) and (2.3) produces the combined free surface boundary condition

$$\left(\frac{\partial}{\partial t}+\vec{U}_0\cdot\nabla\right)^2\Phi + g\frac{\partial\Phi}{\partial z} = 0. \tag{2.17}$$

Substituting the incident velocity potential ϕ_i into (2.17), the dispersion relation for short-crested waves on currents can be derived by applying separation of variables to the differential equation and boundary conditions

$$(\omega-\vec{k}\cdot\vec{U}_0)^2 = \omega^{*2} = gk\tanh kh \tag{2.18}$$

where $\vec{k}=(k_x,k_y)$ are the wave number components in x- and y-axis directions respectively, $k=\sqrt{k_x^2+k_y^2}$, and the relative angular frequency in (2.15) is $\omega^* = \omega - \vec{k}\cdot\vec{U}_0 = \omega - k|\vec{U}_0|\cos(\theta-\beta)$.

From the formula of (2.15) associated with incident waves, we can see that the short-crested waves are propagating in x-axis direction, and varies periodically in y-axis direction. In cylindrical coordinates, the incident wave potential (2.15) can be written as

$$\begin{aligned}\phi_i &= -\frac{igA}{\omega^*}\frac{\cosh k(z+h)}{\cosh kh}\mathrm{e}^{-i\omega t}\left[\sum_{m=0}^{\infty}\varepsilon_m i^m J_m(k_x r)\cos m\theta\right]\left[\sum_{n=0}^{\infty}\varepsilon_n J_{2n}(k_y r)\cos 2n\theta\right]\\ &= -\frac{igA}{2\omega^*}\frac{\cosh k(z+h)}{\cosh kh}\sum_{m=0}^{\infty}\sum_{n=0}^{\infty}\varepsilon_m\varepsilon_n i^m J_m(k_x r)J_{2n}(k_y r)\bigl[\cos(m+2n)\theta+\cos(m-2n)\theta\bigr]\mathrm{e}^{-i\omega t},\end{aligned} \tag{2.19}$$

where $J_m(.)$ is mth order Bessel function of the first kind and ε_m is the Newmann's symbol, $\varepsilon_0 = 1$ and $\varepsilon_m = 2$ for $m \geqslant 1$.

Substituting the total velocity potential $\Phi = \phi_c + \phi_i + \phi_s$ into (2.1)–(2.5), applying the expressions of ϕ_c in (2.12) and ϕ_i in (2.19), the governing equation and boundary conditions for the scattered waves can be written as

$$\Delta\phi_s = \frac{\partial^2\phi_s}{\partial r^2} + \frac{1}{r}\frac{\partial\phi_s}{\partial r} + \frac{1}{r^2}\frac{\partial^2\phi_s}{\partial\theta^2} + \frac{\partial^2\phi_s}{\partial z^2} = 0 \quad -h \leqslant z \leqslant \eta(r,\theta,t), \tag{2.20}$$

$$\left(\frac{\partial}{\partial t} + \vec{U}_0\cdot\nabla\right)^2\phi_s + g\frac{\partial\phi_s}{\partial z} = 0 \quad z = 0, \tag{2.21}$$

$$\frac{\partial\phi_s}{\partial r} = -\frac{\partial\phi_i}{\partial r} - \frac{\partial\phi_c}{\partial r} \quad r = a, \tag{2.22}$$

$$\frac{\partial\phi_s}{\partial z} = 0 \quad z = -h, \tag{2.23}$$

Moreover, the scattered waves must satisfy the Sommerfeld radiation condition at infinity

$$\lim_{kr\to\infty}\sqrt{kr}\left(\frac{\partial}{\partial r} - ik\right)\phi_s = 0. \tag{2.24}$$

In fact, the second term on the right-hand side of (2.22) equals to zero on $r = a$. Similar to the method of Zhu [12], the solution for the scattered waves can be expressed by first satisfying (2.20) and boundary conditions (2.21), (2.23) as

$$\begin{aligned}\phi_s = \frac{igA}{2\omega^*}\frac{\cosh k(z+h)}{\cosh kh}\mathrm{e}^{-i\omega t}\sum_{m=0}^{\infty}\sum_{n=0}^{\infty}\varepsilon_m\varepsilon_n i^m\big[&A_{mn}H_{m+2n}(kr)\cos(m+2n)\theta \\ &+ B_{mn}H_{|m-2n|}(kr)\cos(m-2n)\theta\big],\end{aligned} \tag{2.25}$$

where A_{mn} and B_{mn} are arbitrary constants which can be determined by wall boundary condition (2.22), $H_{m+2n}(kr)$ and $H_{|m-2n|}(kr)$ are the Hankel functions of the first kind that represent outgoing waves. Using the characteristics of Hankel function when $kr \to \infty$

$$H_{m+2n}(kr) \approx \sqrt{\frac{2}{kr}}\exp\left\{i\left[kr - \frac{2(m+2n)-1}{4}\right]\pi\right\},$$

$$H_{|m-2n|}(kr) \approx \sqrt{\frac{2}{kr}}\exp\left\{i\left[kr - \frac{2|m-2n|-1}{4}\right]\pi\right\},$$

the expression (2.25) still satisfies the Sommerfeld radiation condition (2.24). By substituting short-crested incident wave potential ϕ_i of (2.19) and scattered wave potential ϕ_s of (2.25) into side wall boundary condition on the circular cylinder (2.22), the coefficients A_{mn} and B_{mn} can be represented by

$$A_{mn} = \frac{k_x J'_m(k_x a)J_{2n}(k_y a) + k_y J_m(k_x a)J'_{2n}(k_y a)}{kH'_{m+2n}(ka)}, \tag{2.26}$$

$$B_{mn} = \frac{k_x J'_m(k_x a)J_{2n}(k_y a) + k_y J_m(k_x a)J'_{2n}(k_y a)}{kH'_{|m-2n|}(ka)}, \tag{2.27}$$

where the primes denote the differentiation of the Bessel function, $J_n(s)$, or the Hankel function, $H_n(s)$, with respect to their argument s. Thus the total velocity potential Φ can be easily expressed as the sum of the short-crested incident potential $\phi_i(r,\theta,z,t)$, scattered potential $\phi_s(r,\theta,z,t)$ and pure current potential $\phi_c(r,\theta)$

$$\Phi = -\frac{igA}{2\omega^*}\frac{\cosh k(z+h)}{\cosh kh}\mathrm{e}^{-i\omega t}\sum_{m=0}^{\infty}\sum_{n=0}^{\infty}\varepsilon_m\varepsilon_n i^m Q_{mn}(r,\theta) + |\vec{U}_0|\left(r + \frac{a^2}{r}\right)\cos(\theta-\beta) \tag{2.28}$$

in which the function $Q_{mn}(r,\theta)$ is defined as

$$Q_{mn}(r,\theta) = \left[J_m(k_x r)J_{2n}(k_y r) - A_{mn}H_{m+2n}(kr)\right]\cos(m+2n)\theta + \left[J_m(k_x r)J_{2n}(k_y r) - B_{mn}H_{|m-2n|}(kr)\right]\cos(m-2n)\theta. \tag{2.29}$$

Now we have obtained the analytical expressions of total field short crested wave velocity potential with uniform currents. In the followings, the total free surface displacement η, the total horizontal force F_x on the cylinder, the inertia coefficient C_M and drag coefficient C_D will be discussed.

3. Dynamic loading of the cylinder due to short crested waves and currents

Applying total velocity potential (2.28), the free surface wave elevation can be obtained from the linearized dynamic surface condition as

$$\eta = -\frac{1}{g}\frac{\partial \Phi}{\partial t}\bigg|_{z=0} = \frac{A\omega}{2\omega^*}\mathrm{e}^{-i\omega t}\sum_{m=0}^{\infty}\sum_{n=0}^{\infty}\varepsilon_m\varepsilon_n i^m Q_{mn}(r,\theta). \tag{3.1}$$

The dynamic pressure exerted on the cylinder can be determined from the linearized Bernoulli's equation

$$p(a,\theta,z) = -\rho\frac{\partial \Phi}{\partial t} = \frac{\rho g A\omega}{2\omega^*}\frac{\cosh k(z+h)}{\cosh kh}\mathrm{e}^{-i\omega t}\sum_{m=0}^{\infty}\sum_{n=0}^{\infty}\varepsilon_m\varepsilon_n i^m Q_{mn}(a,\theta). \tag{3.2}$$

The total force, per unit length in the direction of wave propagation, is

$$\frac{\mathrm{d}F_x}{\mathrm{d}z} = -a\int_0^{2\pi} p(a,\theta,z)\cos\theta\,\mathrm{d}\theta. \tag{3.3}$$

Thus the total horizontal force on the cylinder, F_x, which can be computed by integrating the expression of (3.3) with respect to z,

$$F_x = \int_{-h}^{0}\frac{\mathrm{d}F_x}{\mathrm{d}z}\,\mathrm{d}z = -\frac{\rho g a A\omega}{2\omega^*}\int_0^{2\pi}\int_{-h}^{0}\frac{\cosh k(z+h)}{\cosh kh}\mathrm{e}^{-i\omega t}\sum_{m=0}^{\infty}\sum_{n=0}^{\infty}\varepsilon_m\varepsilon_n i^m Q_{mn}(a,\theta)\cos\theta\,\mathrm{d}z\,\mathrm{d}\theta. \tag{3.4}$$

Substituting expression $Q_{mn}(a,\theta)$ from (2.29) into (3.4), due to the orthogonality of cosines, the final expression of F_x consists of a single term, which was obtained from the first term in $Q_{mn}(a,\theta)$ with $m=1$, and $n=0$, and a single summation resulted from the second term in $Q_{mn}(a,\theta)$ with $m=2n+1$ and $m=2n-1$,

$$F_x = -\frac{2\pi\rho g A\omega a h}{\omega^*}\frac{\tanh kh}{kh}\mathrm{e}^{-i\omega t}R(k_x,k_y,k,a), \tag{3.5}$$

where

$$R(k_x,k_y,k,a) = i\left[R_0(k_x,k_y,k,a) + \sum_{n=1}^{\infty}R_n(k_x,k_y,k,a)\right] \tag{3.6}$$

and

$$R_0(k_x,k_y,k,a) = J_1(k_x a)J_0(k_y a) - \frac{k_x J_1'(k_x a)J_0(k_y a) + k_y J_1(k_x a)J_0'(k_y a)}{kH_1'(ka)}H_1(ka), \tag{3.7}$$

$$R_n(k_x,k_y,k,a) = i^{2n}\left\{\left[J_{2n+1}(k_x a)J_{2n}(k_y a) - B_{2n+1,n}H_1(ka)\right] - \left[J_{2n-1}(k_x a)J_{2n}(k_y a) - B_{2n-1,n}H_1(ka)\right]\right\}. \tag{3.8}$$

The total moment about an axis parallel to y passing though the bottom of the cylinder is

$$M_y = \int_{-h}^{0}(z+h)\frac{\mathrm{d}F_x}{\mathrm{d}z}\,\mathrm{d}z = -\frac{2\pi\rho g A\omega a h^2}{\omega^*}\frac{kh\sinh kh - \cosh kh + 1}{(kh)^2\cosh kh}\mathrm{e}^{-i\omega t}R(k_x,k_y,k,a). \tag{3.9}$$

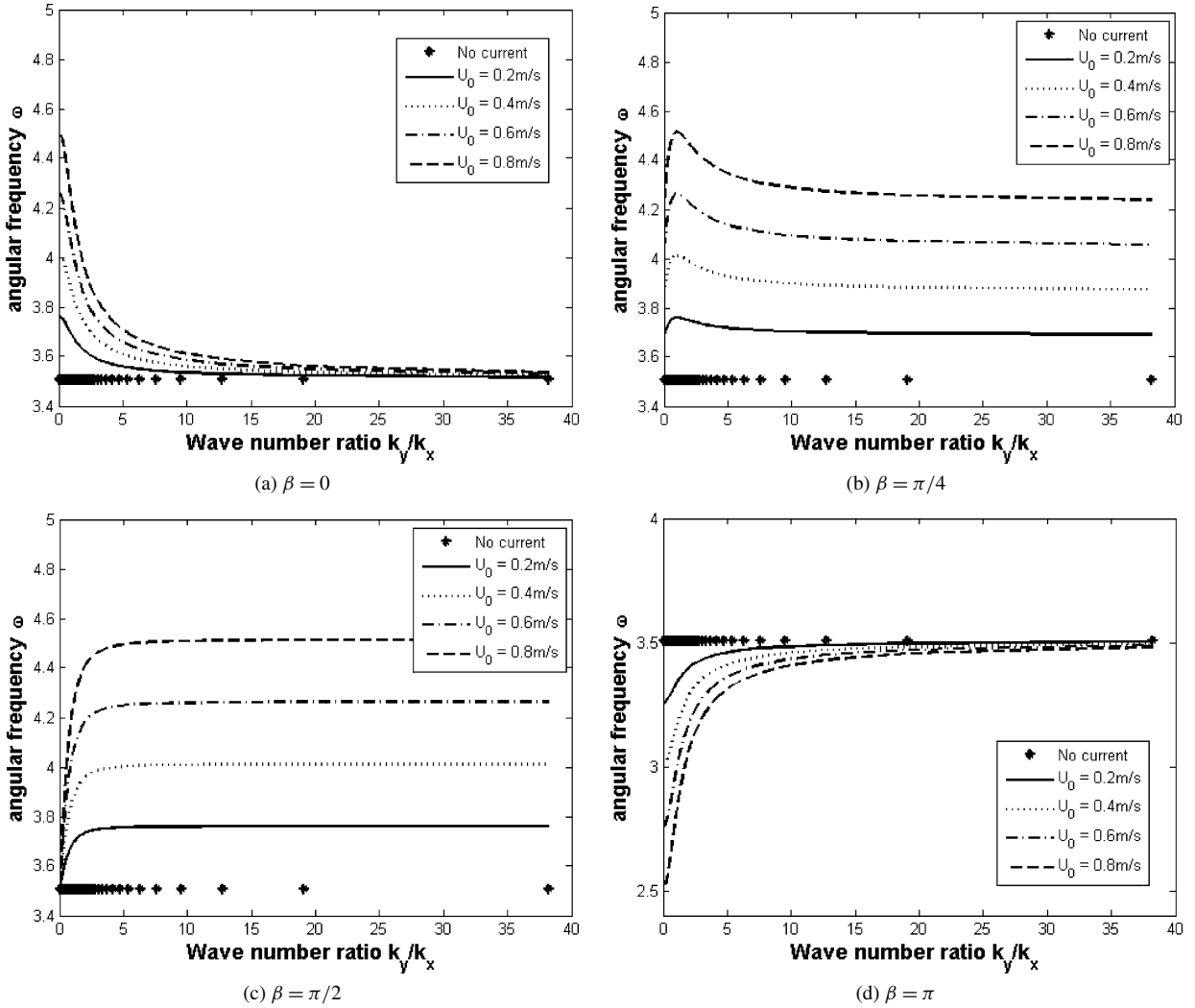

(a) $\beta = 0$ (b) $\beta = \pi/4$

(c) $\beta = \pi/2$ (d) $\beta = \pi$

Fig. 2. Variation of angular frequency ω with wave number ratio k_y/k_x for different incident angle β and current strength ($k = 1.257\ \mathrm{m}^{-1}$, $h = 5$ m).

Following Mei [13], the inertia coefficient C_M and drag coefficient C_D per unit height for the short-crested waves with current can be introduced, which are relate to the added mass and damping coefficient in the restoring forces on a body in forced radiation. For a unit horizontal slice of the cylinder, we have

$$\mathrm{Re}(\mathrm{d}F_x/\mathrm{d}z) = \rho\pi a^2(C_M \partial U/\partial t + \omega C_D U) \tag{3.10}$$

where U is the velocity of the incident short-crested wave at $r = 0$ in the absence of the cylinder. Following Zhu [12], without the constant term $\rho g A \mathrm{e}^{-i\omega t}\cosh k(z+h)/\cosh kh$, total force per unit height can be expressed as

$$\frac{\mathrm{d}F_x}{\mathrm{d}z} \Big/ \left[\rho g A \frac{\cosh k(z+h)}{\cosh kh}\mathrm{e}^{-i\omega t}\right] = \pi k_x a^2 \sqrt{C_M^2 + C_D^2}. \tag{3.11}$$

Thus the inertia coefficient C_M and drag coefficient C_D for the short-crested waves are defined as

$$C_M = -\,\mathrm{Im}\left\{\frac{\mathrm{d}F_x}{\mathrm{d}z} \Big/ \left[\rho g A \frac{\cosh k(z+h)}{\cosh kh}\mathrm{e}^{-i\omega t}\right]\right\} \Big/ \left(\pi a^2 k_x\right),$$

$$C_D = \mathrm{Re}\left\{\frac{\mathrm{d}F_x}{\mathrm{d}z} \Big/ \left[\rho g A \frac{\cosh k(z+h)}{\cosh kh}\mathrm{e}^{-i\omega t}\right]\right\} \Big/ \left(\pi a^2 k_x\right),$$

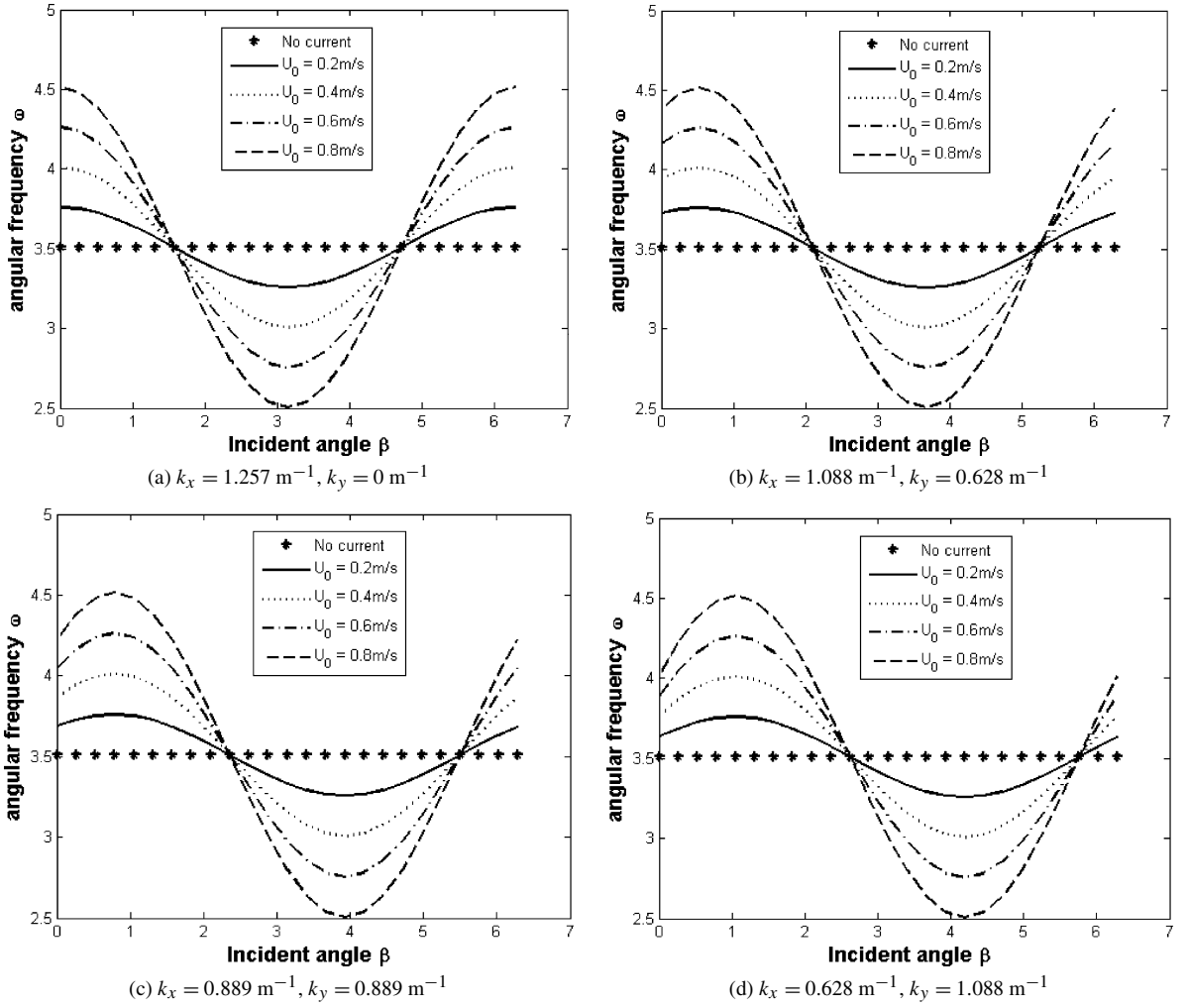

(a) $k_x = 1.257\ \mathrm{m}^{-1}$, $k_y = 0\ \mathrm{m}^{-1}$

(b) $k_x = 1.088\ \mathrm{m}^{-1}$, $k_y = 0.628\ \mathrm{m}^{-1}$

(c) $k_x = 0.889\ \mathrm{m}^{-1}$, $k_y = 0.889\ \mathrm{m}^{-1}$

(d) $k_x = 0.628\ \mathrm{m}^{-1}$, $k_y = 1.088\ \mathrm{m}^{-1}$

Fig. 3. Variation of angular frequency ω with incident angle β of the current for different current strength and wave number components k_x, k_y ($k = 1.257\ \mathrm{m}^{-1}$, $h = 5$ m).

where $\mathrm{Im}[f(x)]$ and $\mathrm{Re}[f(x)]$ represent imaginary and real parts of the function f. After some simplification, the inertia coefficient C_M and drag coefficient C_D can be written as

$$C_M = \frac{2\omega}{k_x a \omega^*}\,\mathrm{Im}\big[R(k_x, k_y, k, a)\big], \qquad C_D = -\frac{2\omega}{k_x a \omega^*}\mathrm{Re}\big[R(k_x, k_y, k, a)\big]. \tag{3.12}$$

4. Computational results and discussion

4.1. The dispersion relation with uniform currents

Dispersion relation is an important relation in the calculation of wave properties. Fig. 2 illustrates the dimensional angular frequency ω as a function of wave number ratio k_y/k_x for different incident angle β and current speed $|U_0|$ using the dispersion relation (2.18). Fig. 2 indicates that the wave frequency increases as current speed increases following positive x-axis direction for a fixed wave number $k = 1.257\ \mathrm{m}^{-1}$ (see Fig. 2 (a), (b) and (c)). However, the wave frequency decreases as current speed increases opposing x-axis direction (see Fig. 2 (d)).

For a fixed wave number $k = 1.257\ \mathrm{m}^{-1}$, Fig. 3 gives the variation of angular frequency ω with incident angle β of the current for different current strength and wave number components k_x, k_y in x- and y-directions. It is known that the currents have no effect on the frequency for plane waves when the current incident angle is 90 degrees from

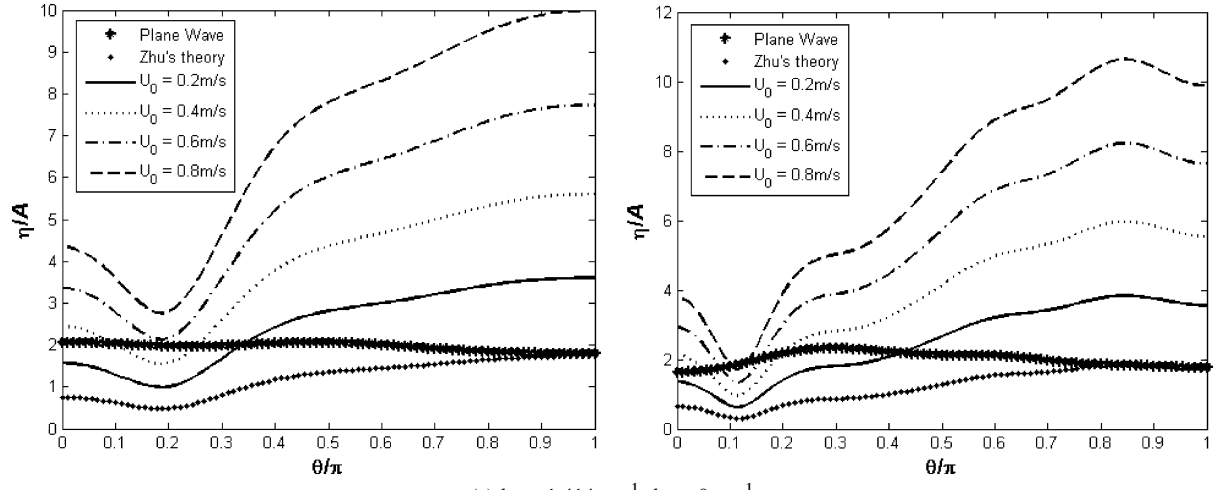

(a) $k_x = 1.414\ \mathrm{m}^{-1}$, $k_y = 0\ \mathrm{m}^{-1}$

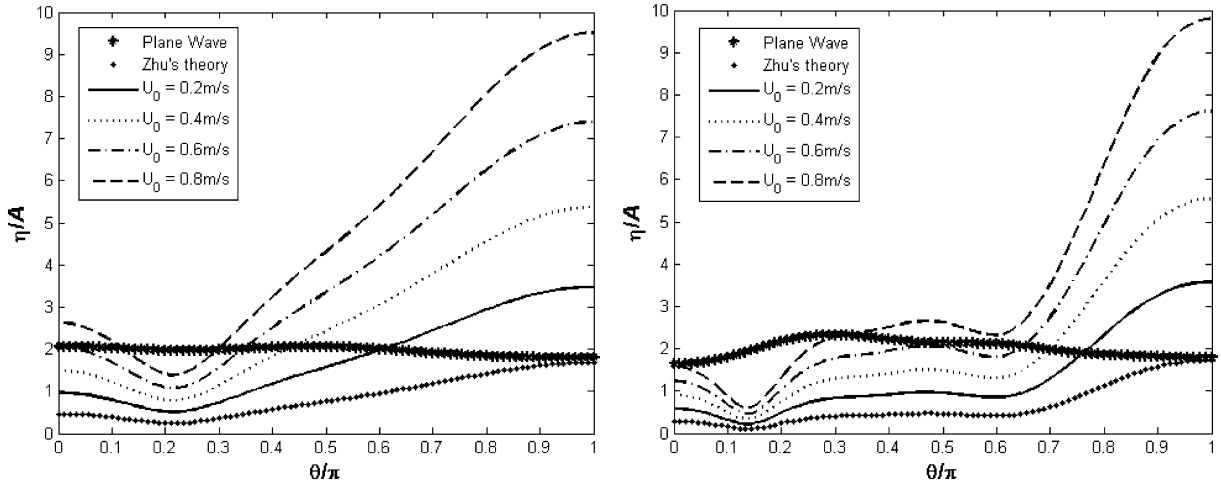

(b) $k_x = 1.225\ \mathrm{m}^{-1}$, $k_y = 0.707\ \mathrm{m}^{-1}$

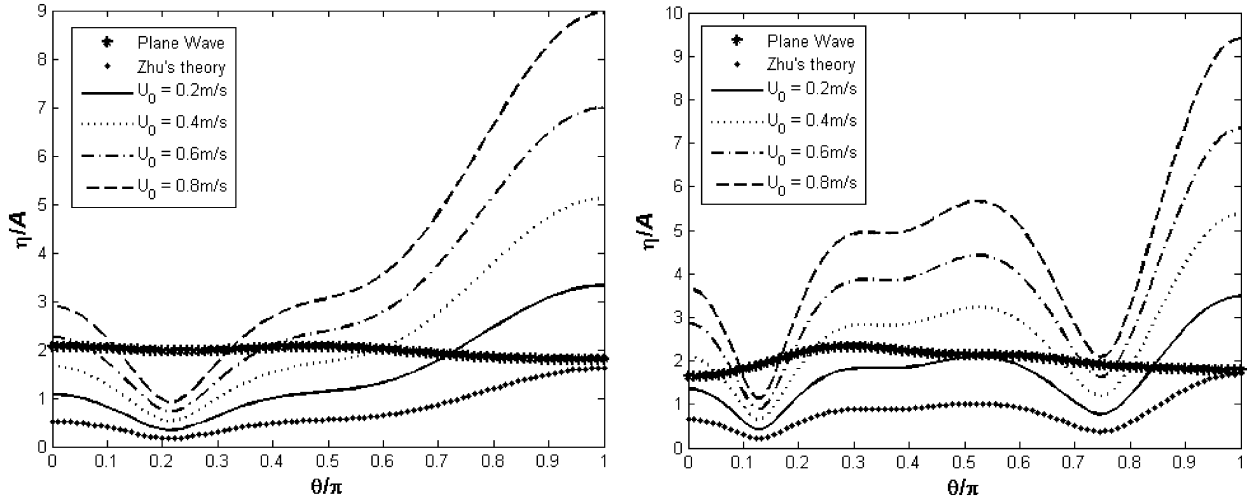

(c) $k_x = 1\ \mathrm{m}^{-1}$, $k_y = 1\ \mathrm{m}^{-1}$

Fig. 4. Short-crested wave run-up of a circular cylinder with radius $a = 1.0$ m (left) and $a = 2.0$ m (right) respectively for different current speed ($\beta = 0$, $h = 5$ m).

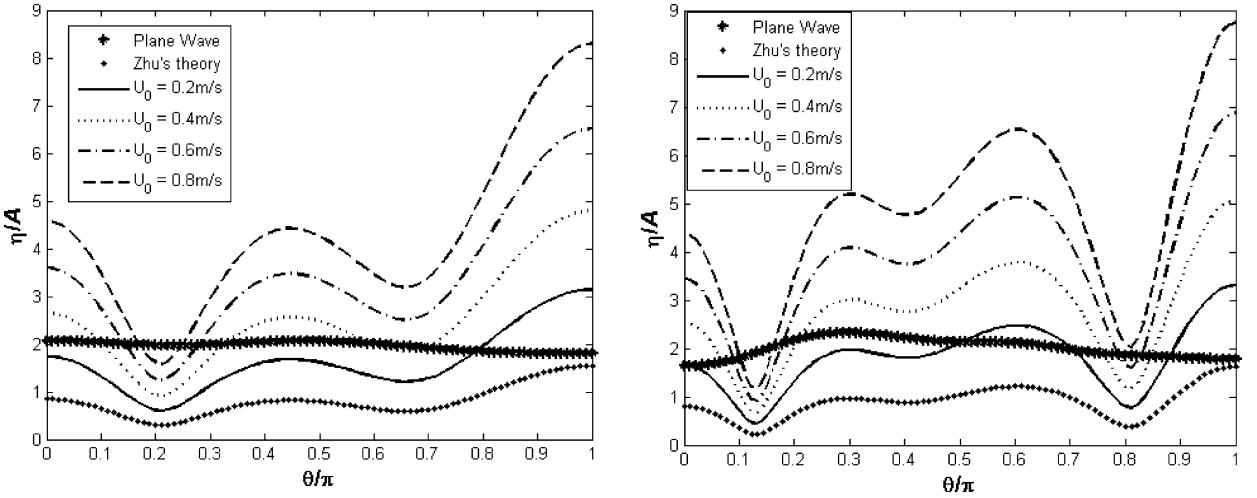

(d) $k_x = 0.707\ \mathrm{m}^{-1}$, $k_y = 1.225\ \mathrm{m}^{-1}$

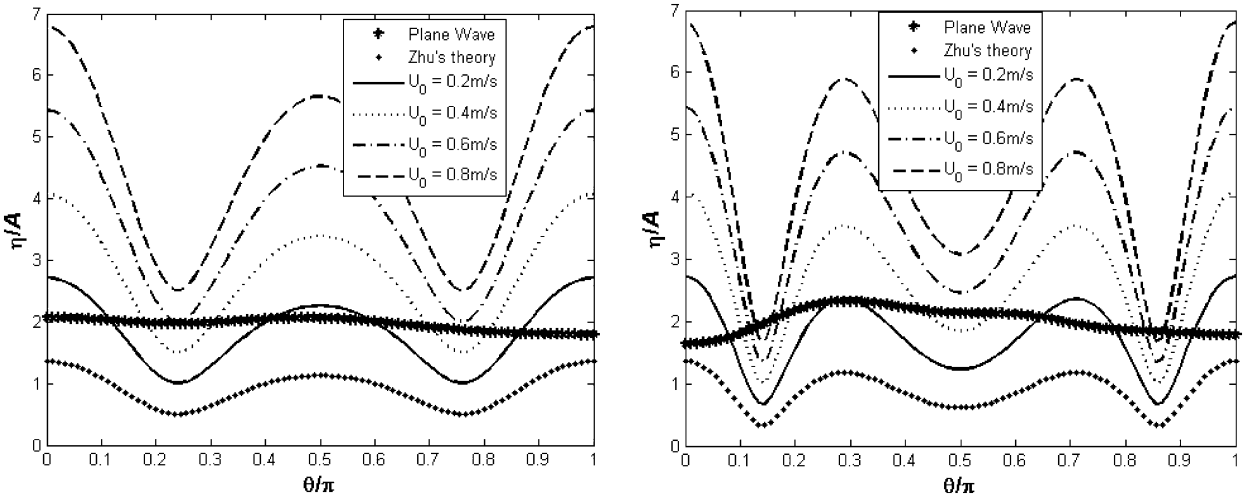

(e) $k_x = 0\ \mathrm{m}^{-1}$, $k_y = 1.414\ m^{-1}$

Fig. 4. *(Continued.)*

the wave propagation direction. Similarly, for the short-crested wave in Fig. 3, when the current incident angle is 90 degrees from the wave propagation direction, for example, $\alpha - \beta = \pi/2$ (where α is the wave propagation direction), the currents have no effect on wave frequency. It still can be seen from Fig. 3 (a)–(d) that as the incident waves gradually become short-crested, the frequency peaks and valleys change periodically. These peaks and valleys are related to the conditions $\alpha - \beta = 0$ and $\alpha - \beta = \pi$ respectively. This can be easily seen from the dispersion relation (2.18). Physically, the frequency peaks and valleys describe the situation when current incident angle parallels and inverses to the direction of the wave propagating respectively.

4.2. The wave run-up of a cylinder with uniform currents

Concerning to the numerical techniques, since the above analytical expressions were given in terms of infinite sums, they were truncated at some finite order in our computation for the following results. In fact, we let both m and n equal to 5, because all the results when m and n are larger than 5 will convergence and stable.

A series of numerical experiments at a fixed time are shown in Fig. 4 to investigate the dimensionless run-up η/A of short-crested waves on a bottom-mounted vertical circular cylinder against variable θ/π with and without currents for

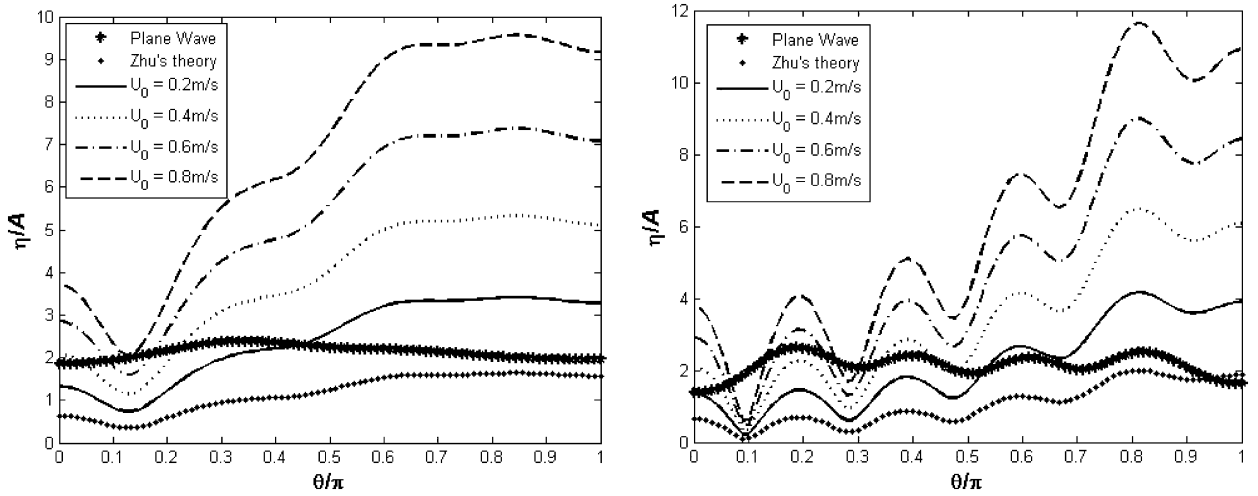

(a) $k_x = 2.236\ \mathrm{m}^{-1}$, $k_y = 0\ \mathrm{m}^{-1}$

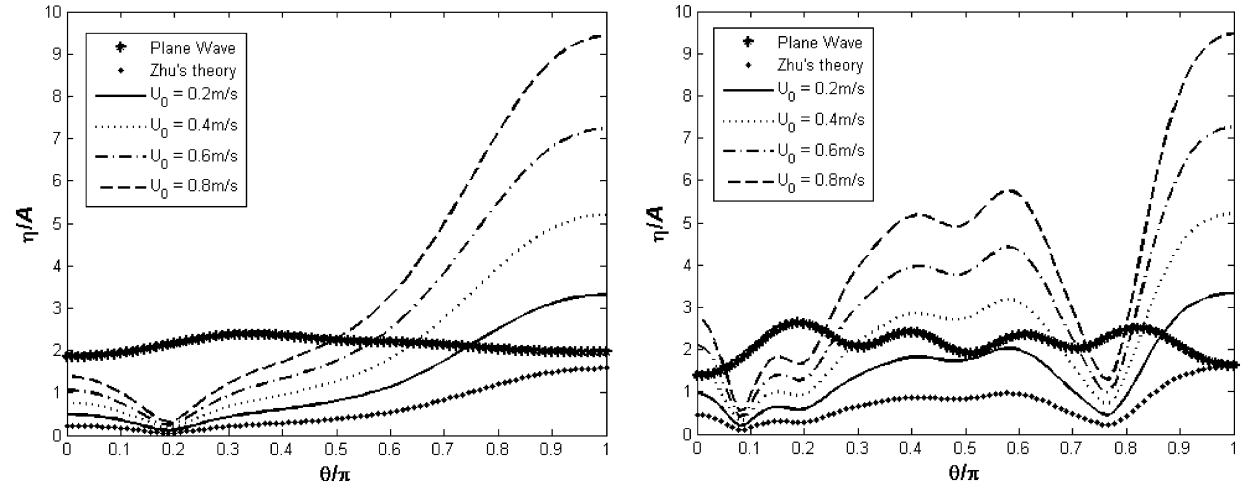

(b) $k_x = 1.937\ \mathrm{m}^{-1}$, $k_y = 1.118\ \mathrm{m}^{-1}$

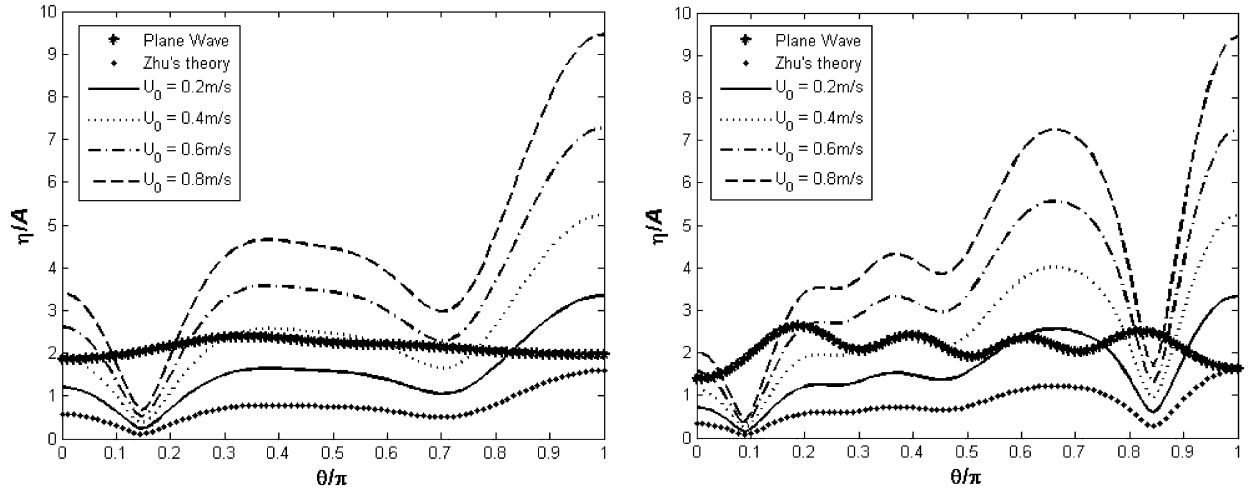

(c) $k_x = 1.581\ \mathrm{m}^{-1}$, $k_y = 1.581\ \mathrm{m}^{-1}$

Fig. 5. The variation of the short-crested wave run-up on a circular cylinder versus θ/π with radius $a = 1.0$ m (left) $a = 2.0$ m (right) respectively for different current speed ($\beta = \pi/6$, $h = 5$ m).

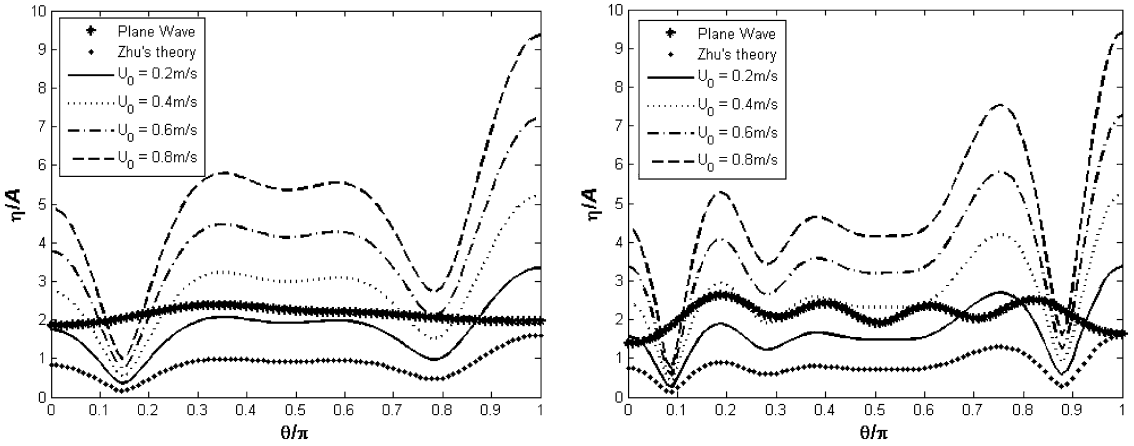

(d) $k_x = 1.118\ \mathrm{m}^{-1}$, $k_y = 1.937\ \mathrm{m}^{-1}$

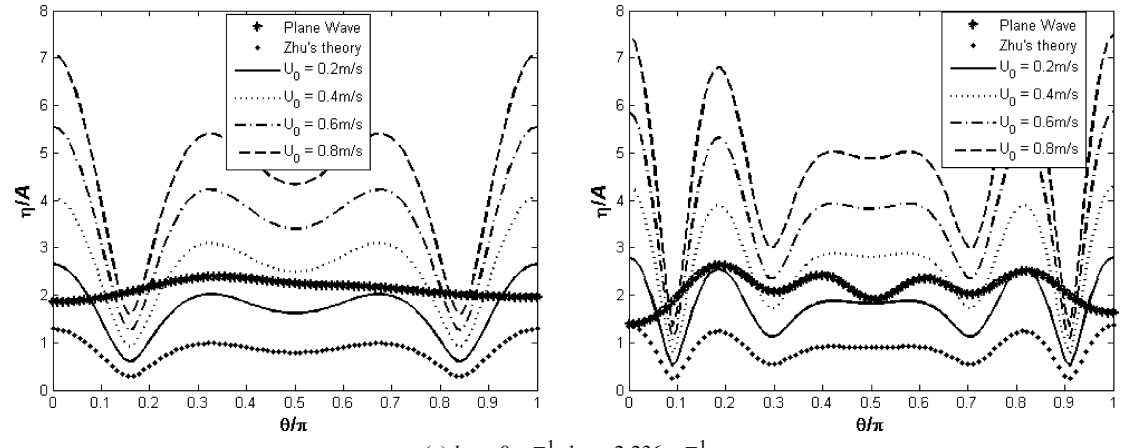

(e) $k_x = 0\ \mathrm{m}^{-1}$, $k_y = 2.236\ \mathrm{m}^{-1}$

Fig. 5. *(Continued.)*

different radius of the cylinder. The direction of a current is assumed following incident short-crested wave direction. The left- and right-hand sides of Fig. 4 are corresponding to radius of 1 m and 2 m cylinder respectively.

From Fig. 4 it is seen that the location of the maximum run-up on the cylinder is at the front of the cylinder. Increasing the current speed results in an increase in the run-up on the cylinder. For fixed total wave number $1.414\ \mathrm{m}^{-1}$, when the wave number in x-axis direction decreases (for example, the incident wave changes from long crested plane waves to short-crested waves), the wave amplitude decreases and diffraction effects become more and more pronounced. When k_x becomes zero and $k_y = k$, the amplitude of the waves on the front side of the cylinder reduced to a minimum. Under this circumstance, the incident short-crested wave gives a standing wave in y-direction, and thus the water run-up is symmetric in θ direction in Fig. 4 (e) for different current strength. A minimum amplitude (for example, the valley of water run-up) exists between the two extremes of $k_x = k$ and $k_y = k$. The reason is maybe that in this θ location, $Q_{mn}(r, \theta)$ in (2.29) attains minimum value. Furthermore, by comparing the results of 1 m cylinder radius with those of 2 m cylinder radius, we find that the water run-up on the front of the cylinder increases as the increase of radius of the cylinder.

Similar to Fig. 4, Fig. 5 illustrates the water run-up on a cylinder when the total wave number is equal to $2.236\ \mathrm{m}^{-1}$, incident angle of the current is equal to $\pi/6$. It can be noted from Fig. 5 that the water run-up in the case of large wave number with different currents is smaller than that in small wave number case in Fig. 4.

Moreover, it can still be proved from Figs. 4 and 5 that the run-up of short-crested wave without current is smaller than that of long crested plane wave as in Ref. [12]. It is, however, very interesting to note that when the current presents, the run-up with even small current speeds will exceed the corresponding run-up for pure short crested wave both on the front of the cylinder and many other locations in θ direction.

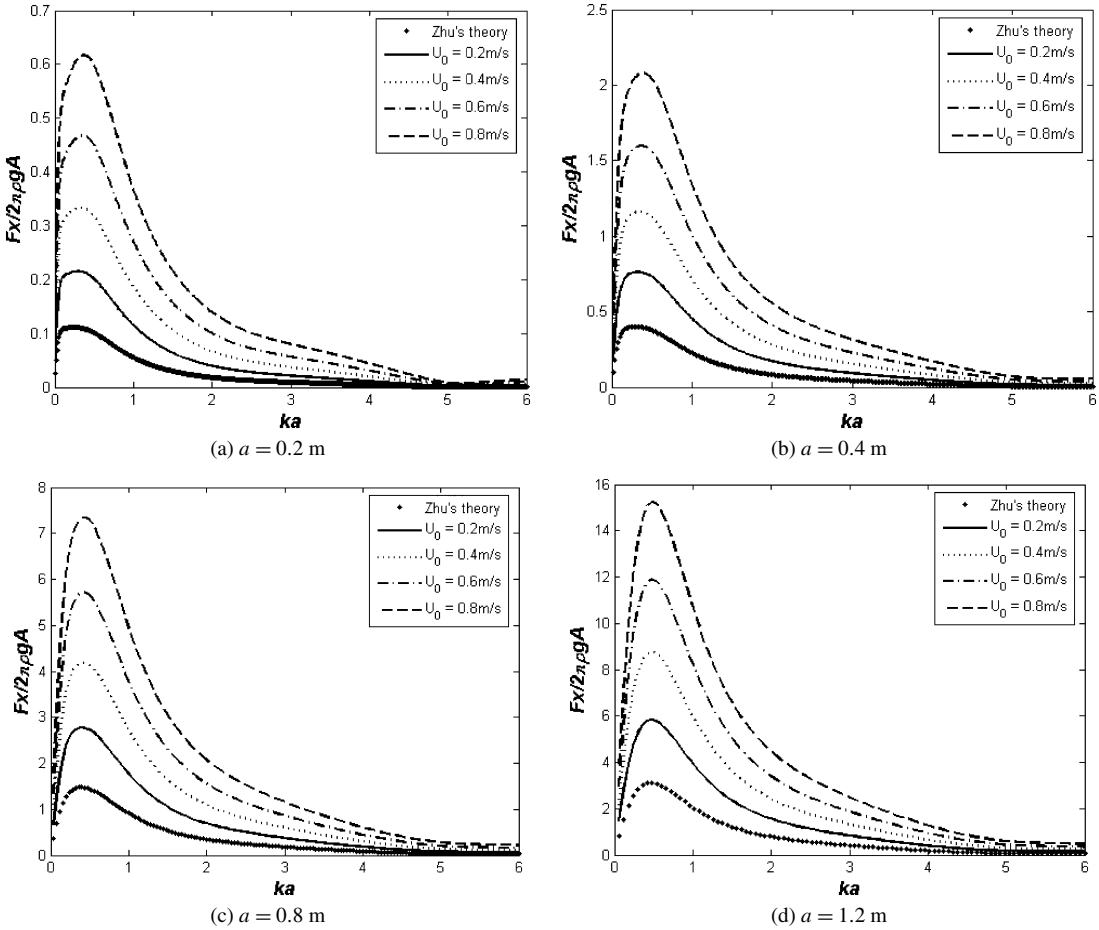

(a) $a = 0.2$ m (b) $a = 0.4$ m

(c) $a = 0.8$ m (d) $a = 1.2$ m

Fig. 6. The variation of the total horizontal short-crested wave force on a circular cylinder versus the ka for different current speed and cylinder radius ($\beta = \pi/6$, $h = 5$ m).

4.3. The short-crested wave force on a cylinder with uniform currents

Fig. 6 illustrates the variation of the total horizontal short-crested wave force on a circular cylinder versus the ka with different currents speed for different radius of the cylinder. In Fig. 6, regardless of the values of current speed and radius of the cylinder, the wave force attains a maximum at low frequency, then decays gradually. The wave force increases obviously as the increase of current speed. Moreover, the larger of the radius of the cylinder, the larger of the wave force is.

The signs of C_M and C_D in Eq. (3.12) depend largely on the real and image parts of the expression $R(k_x, k_y, k, a)$ in Eq. (3.6). McIver and Evans [14] has related the added mass and damping to the energy of the fluid motion. They found that the negative added mass and damping occur when the body is oscillating sufficiently close to the free surface. The variation of the inertia coefficient C_M and drag coefficient C_D on a circular cylinder versus the ka with different current speeds for different radius of the cylinder is shown in Fig. 7. The conclusion can be drawn from Fig. 7 that the inertia and drag coefficients increase obviously with the increase of current speed. It should be noted that at certain intervals of ka, such as $1.8 < ka < 5$, the damping coefficient on a cylinder is negative, which probably means that an increase of the vibratory amplitude for circular cylinder to be expected in these intervals under prescribed conditions due to interaction of the short-crested wave and oblique currents. Moreover, the sharp peak of inertia coefficient in the curves displayed in Fig. 7 suggests that there is an approximate resonant motion at a low frequency (or small ka). The resonance will occur when the denominator $kH_1'(ka)$ of $R(k_x, k_y, k, a)$ in Eq. (3.6) tends to zero.

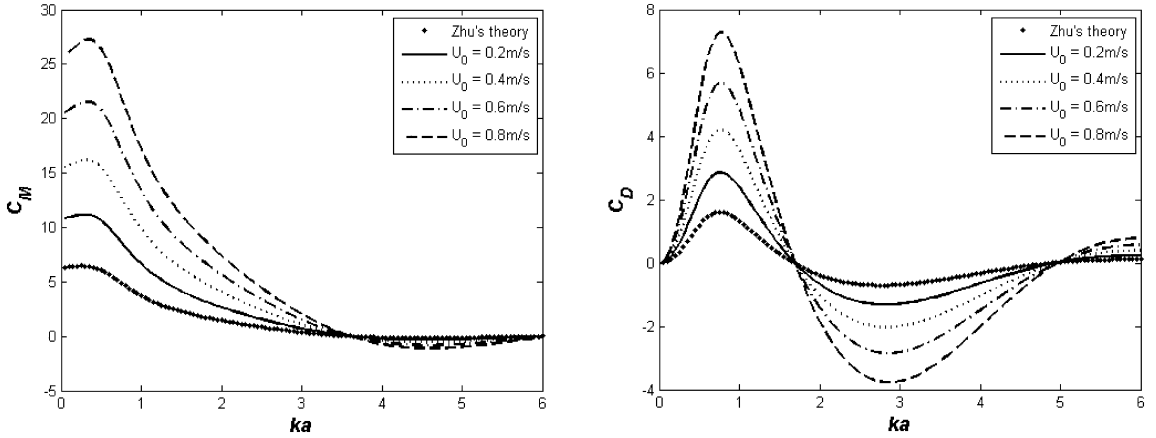

(a) $a = 1.0$ m

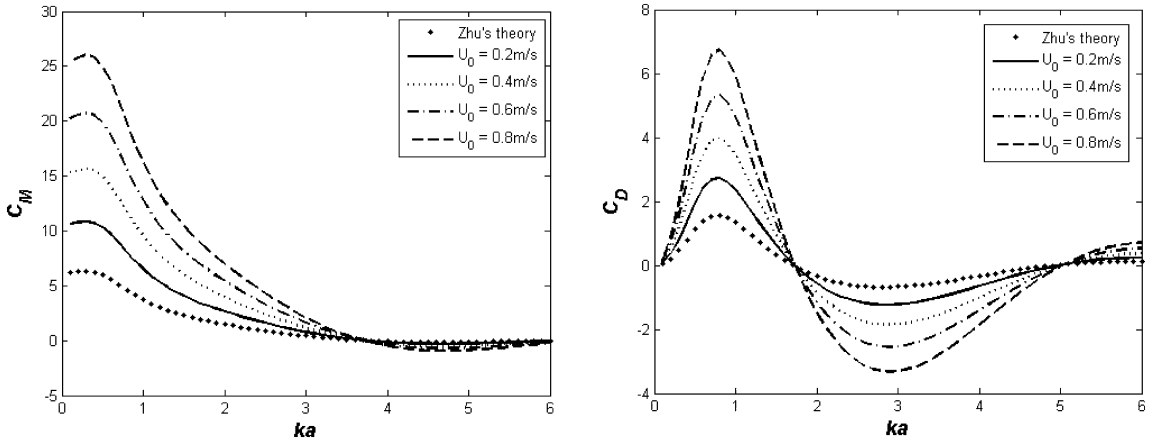

(b) $a = 2.0$ m

Fig. 7. The variation of the inertia coefficient C_M and drag coefficient C_D on a circular cylinder versus the ka for different current speed and cylinder radius ($\beta = \pi/6$, $h = 5$ m).

5. Conclusions and discussion

In this study, a new analytical solution for the short crested waves with currents around a bottom-mounted large circular cylinder was derived. Some numerical results of the new solution was obtained by comparing the results of wave run-up on a cylinder with those of Zhu [12]. With the new solution, the important influences of currents on the wave run-up, wave frequency, wave force, and inertia and drag coefficients have been demonstrated. Based on the numerical results presented, the following conclusions can be drawn:

(1) Wave frequency of short crested wave system is affected by current incident angle and the strength of the currents. The wave frequency increases as current speed increases following wave propagating direction for a fixed wave number. However, the wave frequency decreases as current speed increases opposing x-axis direction.
(2) With the increase of current speed, the water run-up on the cylinder becomes higher, which can be larger than that of long crested plane wave and short crested wave case without currents even though the current speed is small.
(3) The total wave loads, inertia coefficient and drag coefficient exerted on a cylinder with currents would be larger compared to the wave loads exerted pure short-crested waves. For large marine construction, the influence of currents is pronounced. Thus ocean engineers should consider the short crested wave–current load on marine constructs carefully.

An efficient boundary element method to calculate the wave loads induced by plane waves on vertical cylinders were proposed (for example, Au and Brebbia [15]). Zhu and Moule [16] expended this approach to calculated the wave loads, induced by short-crested incident waves, on a vertical cylinder of arbitrary cross-section. They found that for a cylinder of elliptical cross-section, the wave loads induced by short-crested waves can be larger than those induced by plane waves with the same total wave number. However, they did not consider the run-up and forces of short-crested wave and current interaction on a cylinder. As we know, under steady current condition, the run-up is insignificant and forces are absent within the frame of potential theory. However, superposition of moderate current and waves leads to significant increase of wave run-up and forces. The reason is mainly that when water waves approaching a uniform current at an angle, the wavelength, steepness and propagating direction of the waves will change due to the refractive effects and the work being done by a steady uniform current against the radiation stress of the waves. The amplification mechanism of run-up on a cylinder is that the amplitude of surface waves is affected by a nonlinear interaction between the waves and the current.

we demonstrated the theoretical analysis based upon the potential flow, and did not consider the flow separation and turbulence. In ocean engineering practices, however, the wave motion in upper ocean is strongly turbulent rather than regular short-crested. Thus models based on the potential flow theory have limited applications. To represent the physical situation more precisely, a large eddy simulation (LES) solver to Navier–Stokes equations with the appropriate turbulence closure model is proposed by Lin and Li [17]. They studies the wave–current interaction with a vertical square cylinder. Additional studies on the effect of short-crested wave or wave–current interaction on the fluid loading of large offshore structures may be conducted by LES method in this fields for future research.

Acknowledgements

The authors are grateful for the support of opening fund from Guangdong Province Key Laboratory of Coastal Ocean Engineering, the National Natural Science Foundation of China (Grant No: 10102024, 10572154). Meanwhile, this work is supported by Program for New Century Excellent Talents in University, NCET-06-0731, the foundation of Sun Yat-sen University Advanced Research Center, and the support from for the start up fund for young teachers in Zhongshan University. The authors still would like to thank the referees for their invaluable suggestions and for their help in modifying the paper.

References

[1] J.R. Morison, M.P. O'Brien, J.W. Johnson, S.A. Schaaf, The forces exerted by surface wave on piles, Petrol. Trans. AIME 189 (1950) 149–154.
[2] R.C. MacCamy, R.A. Fuchs, Wave forces on piles: a diffraction theory, US Army Corps of Engineering, Beach Erosion Board, Technical Memorandum No. 69 (1954).
[3] S. Neelamani, V. Sundar, C.P. Venohan, Dynamic pressure distribution on a cylinder due to wave diffraction, Ocean Eng. 16 (1989) 343–353.
[4] S.K. Chakrabatri, A. Tam, Interaction of waves with large vertical cylinder, J. Ship Res. 19 (1975) 22–33.
[5] P. Bettess, O.C. Zienkiewicz, Diffraction and refraction of surface waves using finite and infinite elements, Int. J. Num. Meth. Eng. 11 (1976) 1271–1290.
[6] T.-K. Tsay, W. Zhu, P.L.-F. Liu, A finite element model for wave refraction, diffraction, reflection and dissipation, Appl. Ocean Res. 11 (1989) 33–38.
[7] C.C. Tung, N.E. Huang, Influence of wave–current interactions on fluid force, Ocean Eng. 2 (1973) 207–218.
[8] R.K. Watanabe, The effect of wave–current interactions on the hydrodynamic loading of large offshore structures, PhD Thesis, Graduate College of Texas A&M University, 1982.
[9] J.R.C. Hsu, Y. Tsuchiya, R. Silvester, Third-order approximation to short-crested waves, J. Fluid Mech. 90 (1979) 179–196.
[10] R. Silvester, J.R.C. Hsu, Sines revisited, J. Waterway Port Coastal Ocean Eng. ASCE 115 (1989) 66–85.
[11] H. Huang, F. Jia, The patterns of surface capillary-gravity short-crested waves with uniform current fields in coastal waters, Acta Mech. Sinica 22 (2006) 433–441.
[12] S.P. Zhu, Diffraction of short-crested waves around a circular cylinder, Ocean Eng. 20 (4) (1993) 389–407.
[13] C.C. Mei, The applied dynamics of ocean surface waves, in: World Scientific, 1989, pp. 315–316.
[14] P. McIver, D.V. Evens, The occurrence of negative added mass in free-surface problems involving submerged oscillating bodies, J. Eng. Math. 18 (1984) 7–22.
[15] M.C. Au, C.A. Brebbia, Diffraction of water waves for vertical cylinders using boundary elements, Appl. Math. Modelling 7 (2) (1983) 106–114.
[16] S.P. Zhu, G. Moule, Numerical calculation of forces induced by short-crested waves on a vertical cylinder of arbitrary cross-section, Ocean Eng. 21 (7) (1994) 645–662.
[17] P.Z. Lin, C.W. Li, Wave–current interaction with a vertical square cylinder, Ocean Eng. 30 (7) (2003) 855–876.